

# Comparison of the Characteristics of Adsorption Equilibrium and Surface Diffusion in Liquid–Solid and Gas–Solid Adsorption on C<sub>18</sub>-Silica Gels

Kanji Miyabe<sup>†</sup> and Georges Guiochon<sup>\*‡</sup>

Department of Applied Chemistry, Nagoya Institute of Technology, Gokiso, Showa, Nagoya 466-8555, Japan, and Department of Chemistry, The University of Tennessee, Knoxville, Tennessee 37996-1600, and Division of Chemical Sciences, Oak Ridge National Laboratory, Oak Ridge, Tennessee 37831

Received: July 30, 2003; In Final Form: December 5, 2003

Four parameters characterizing the adsorption equilibrium, surface diffusion, and related thermodynamic properties were derived from pulse-response experiments in various reversed-phase liquid chromatography (RPLC) systems using C<sub>18</sub>-silica gels and aqueous solutions of three different organic modifiers, methanol, acetonitrile, and tetrahydrofuran. The results were compared with corresponding data similarly measured by gas–solid chromatography on the same type of surface-modified silica gel, with helium. Information on the solvent effect on the adsorption characteristics was provided by the comparison of these experimental results. While the adsorption equilibrium constant and the heat of adsorption at infinite dilution were much larger in the gas–solid than in the RPLC system, the surface diffusion coefficient ( $D_s$ ) and the activation energy of surface diffusion ( $E_s$ ) were of the same order of magnitude in both systems. Regarding surface diffusion, the logarithm of the frequency factor was linearly correlated with  $E_s$  by the same straight line, suggesting the fundamental similarity of the surface diffusion mechanism in the gas–solid and liquid–solid systems. Calculations made on the basis of a surface-restricted diffusion model provide an explanation for the comparable values of  $D_s$  and  $E_s$  in the two systems. In conclusion, the liquid phase in RPLC influences the thermodynamic parameters of surface diffusion as well as those of adsorption equilibrium, but similar values of  $D_s$  and  $E_s$  are observed in both the two adsorption systems. A quantitative explanation of the similarities and differences of the characteristics and the mechanism of surface diffusion in gas–solid and liquid–solid adsorption systems is proposed.

## Introduction

The solvents used to make the mobile phase have an extremely important influence on the separation achieved in liquid chromatography. The wide range of possible choices regarding the composition of the mobile phase is the essential reason liquid chromatography is widely viewed as the most effective separation technique for both analytical and preparative applications.<sup>1</sup> The nature of the organic modifier and the composition of the mobile phase can be chosen arbitrarily, depending on the purpose and the difficulty of the intended separation.<sup>2,3</sup> In reversed-phase liquid chromatography (RPLC), aqueous solutions of organic modifiers, such as methanol, acetonitrile, and tetrahydrofuran (THF), are conventionally used as modifiers.

The influence of the mobile phase composition on the chromatographic behavior in RPLC has been abundantly studied from the viewpoints of adsorption equilibrium and related thermodynamic properties.<sup>4</sup> The retention characteristics in RPLC were described by considering the hydrophobic effect (the solvophobic theory)<sup>2,5–8</sup> and by using the partition model.<sup>9–12</sup> For instance, Horváth et al. quantitatively explained the hydrophobic interactions between the sample molecules and the surface of the stationary phase in RPLC.<sup>5</sup> The solvophobic theory was also applied to study the adsorptivity of organic compounds from aqueous solutions onto activated carbon<sup>13</sup> and

to explain the characteristic features of the liquid–liquid extraction equilibrium of ion pairs.<sup>14</sup> In the solvophobic theory,<sup>2,5–8</sup> it is assumed that the adsorption of the liquid phase can be divided into two conceptual processes on the basis of a cyclic thermodynamic model. One step is the gas-phase adsorption of the adsorbate onto the adsorbent, in the absence of solvent. The other step is the solvation of all the chemical species involved in adsorption. The liquid-phase adsorption is analyzed by referring to adsorption in a corresponding gas system, in which no influence of the solvent on adsorption must be taken into account.

It is obvious that the chromatographic behavior depends on the characteristics of both the adsorption equilibrium and the mass-transfer kinetics.<sup>1,15</sup> However, there are few detailed studies on kinetic processes in RPLC systems, especially on the mass transfer inside the particles, in contrast with the abundance of fundamental investigations on the retention behavior. Among several mass-transfer processes in chromatographic columns, surface diffusion is a most informative kinetic process because it consists of molecular migration in the adsorbed state.<sup>15,16</sup> The surface diffusion process should be affected by the adsorption behavior of the sample because it takes place in the potential field of the surface. The characteristics of surface diffusion reflect the choice of RPLC conditions such as the physicochemical properties of the mobile phase and the sample compounds. Some experimental studies have been carried out on surface diffusion or lateral diffusion in RPLC.<sup>17–20</sup> Although they provide experimental data concerning surface or lateral diffusion for a few systems, no systematic interpreta-

\* Author to whom correspondence may be addressed. E-mail: guiochon@utk.edu.

<sup>†</sup> Nagoya Institute of Technology.

<sup>‡</sup> University of Tennessee.

**TABLE 1: Properties of C<sub>18</sub>-Silica Gel Columns and Experimental Conditions**

mobile phase/carrier gas	liquid–solid (RPLC) systems			gas–solid system
	methanol/water (70/30, v/v)	acetonitrile/water (70/30, v/v)	THF/water (50/50, v/v)	helium
superficial velocity, $u_0$ (cm s <sup>-1</sup> )	0.06–0.12	0.06–0.12	0.06–0.12	7.1–14.1
average diameter of the stationary phase particles, $d_p$ (μm)	45	45	54	296
particle density, $\rho_p$ (g cm <sup>-3</sup> )	0.86	0.81	0.82	0.95
particle internal porosity, $\epsilon_p$	0.46	0.37	0.29	0.37
tortuosity factor, $k^2$	4.5	5.5	4.0	8.4
carbon content (wt %)	17.1	17.1	14.9	19.8
base silica gel specific surface area (m <sup>2</sup> g <sup>-1</sup> )	290	290	340	ND <sup>a</sup>
C <sub>18</sub> -silica gel specific surface area (m <sup>2</sup> g <sup>-1</sup> )	180	180	ND <sup>a</sup>	160
column external porosity, $\epsilon$	0.43	0.39	0.40	0.31
column size (mm)	6 × 150	6 × 150	6 × 150	3.2 × 195
column temperature (K)	288–308	288–308	288–308	313–418

<sup>a</sup> Not detected.

tions of the intrinsic characteristics and the mechanism of surface diffusion in RPLC seem to have been attempted, yet.

Previously, we reviewed surface diffusion data measured by moment analysis of pulse-response experiments in RPLC, under various experimental conditions (e.g., with different compounds and stationary/mobile phase systems) and in a gas–solid chromatography using C<sub>18</sub>-silica gel as the adsorbent.<sup>21</sup> Some characteristic features of surface diffusion in RPLC were clarified from both kinetic and thermodynamic points of view. Surface diffusion was shown to be the predominant contribution in the intraparticle migration of the sample molecules through C<sub>18</sub>-silica gel particles, in both gas–solid and liquid–solid systems.<sup>21,22</sup> The dependence of the surface diffusion coefficient ( $D_s$ ) on the adsorbate concentration was studied.<sup>21,23</sup> The value of  $D_s$  increases with increasing amount adsorbed. The positive concentration dependence of  $D_s$  was accounted for in terms of the chemical potential driving force model. Analyses of the temperature dependence of  $D_s$  provided information on the thermodynamic properties of surface diffusion. Extrathermodynamic correlations, e.g., enthalpy–entropy compensation<sup>21,24–27</sup> and linear free energy relationships,<sup>21,24,25,27,28</sup> concerning surface diffusion were established.

We also studied the dependence of  $D_s$  of homologous series on their retention strength. The value of  $D_s$  tends toward the molecular diffusivity ( $D_m$ ) with decreasing energy of adsorptive interactions between sample molecules and the stationary phase surface, suggesting a form of correlation between surface diffusion and molecular diffusivity and that the variation of  $D_s$  depends primarily on that of  $D_m$ .<sup>21,29</sup> Surface diffusion was regarded as a molecular migration phenomenon restricted in the potential field of adsorption. We derived a surface-restricted molecular diffusion model as a first approximation for the mechanism of surface diffusion and formulated this model on the basis of the absolute rate theory.<sup>21,24,25,28–30</sup> It is effective for a comprehensive interpretation of the intrinsic characteristics and the mechanism of surface diffusion in liquid–solid adsorption systems.

In the solvophobic theory,<sup>2,5–8,21</sup> as described earlier, the retention equilibrium in RPLC systems is analyzed by dividing the liquid–solid adsorption phenomenon into two processes, i.e., the gas–solid adsorption and the solvation of all the chemical species concerned. It is expected that a comparison of experimental data on surface diffusion in gas–solid and in liquid–solid adsorption systems can provide information on the characteristics and mechanism of surface diffusion. So far, only a few authors have discussed the correlation of diffusion

phenomena in gas–solid and liquid–solid systems, even in the cases of important adsorbents such as activated carbons or zeolites.<sup>16,31</sup> This paper is concerned with the solvent effect on the adsorption characteristics and mainly on surface diffusion. The adsorption equilibrium and the mass-transfer phenomena in RPLC were taken as one concrete example.

First, the influence of the mobile phase solvents on the adsorption equilibrium, the mass-transfer kinetics, and related thermodynamic properties is experimentally clarified. The values of characteristic parameters measured in the RPLC system were compared with those obtained for the corresponding gas–solid system. Then, an enthalpy–entropy compensation regarding surface diffusion is discussed in connection with the similarity of the mechanisms. Finally, hypothetical calculations were made on the basis of a surface-restricted diffusion model for surface diffusion in order to quantitatively explain the comparable values of  $D_s$  and  $E_s$  obtained in the gas–solid and RPLC systems. On the basis of these results, the characteristic features and the mechanism of surface diffusion are discussed.

## Experimental Section

**Column and Reagents.** The physicochemical properties of the C<sub>18</sub>-silica gel particles (YMC, Kyoto, Japan) and the parameters of the columns used are reported in Table 1. The packing materials are made by covalently bonding monofunctional *n*-octadecyldimethylsilyl ligands onto the surface of a conventional silica gel. Most of the information on the packing materials and columns was provided by the manufacturer and the rest determined by nitrogen adsorption and by scanning electron microscopy.

In liquid–solid adsorption experiments, commercially available packed columns were used. The particle diameter ( $d_p$ ) of the C<sub>18</sub>-silica gel particles was 45 or 54 μm. The particle size is relatively large compared to that of packing materials conventionally used for analytical separations. Relatively large C<sub>18</sub>-silica gels were used in order to make easier the quantitative analysis of band broadening phenomena and, more specifically, the accurate estimate of the parameters of surface diffusion.

Aqueous solutions of three organic modifiers, methanol, acetonitrile, and THF, were used as the mobile phase. Water was prepared by the distillation of ion-exchanged water. The volumetric compositions of methanol, acetonitrile, and THF in the mobile phase solvents were adjusted to 70, 70, and 50%, respectively, because, with 70% v/v of THF in the mobile phase, the retention of the sample compounds was too small for the accurate measurement of the parameters of their adsorption and

mass-transfer kinetics. A nomograph for the elution strength of aqueous solutions in RPLC indicates that the elution strength of a 50% v/v aqueous solution of THF is approximately the same as those of 70–80% v/v methanol or 60–70% v/v acetonitrile aqueous solutions.<sup>3</sup> Although this correlation is not rigorous, the choice of the mobile-phase composition is reasonable because the elution strength of the different solutions used was comparable and, in this study, we wanted to compare the characteristics of the adsorption equilibrium and surface diffusion in RPLC systems with those in corresponding gas–solid adsorption system, using the same type of packing material.

The sample compounds were all reagent grade and were used without further purification. Sample solutions were prepared by dissolving the sample compounds into the mobile phase. The concentration of the sample compound was about 0.1% w/w in most cases. Uracil and sodium nitrate were used as inert tracers. The elution peaks of inert tracers were analyzed in order to derive information on the physical parameters of the stationary phase particles and of the columns, i.e., the internal porosity of the C<sub>18</sub>-silica gel particles ( $\epsilon_p$ ), the tortuosity factor of the pores ( $k$ ), and the external porosity of the column ( $\epsilon_e$ ).

In the gas–solid adsorption experiments, a homemade column was prepared by packing C<sub>18</sub>-silica gel particles ( $d_p = 296 \mu\text{m}$ ) into a glass tube. Helium (purity ca. 99.9%) was used as the carrier gas. Alkylbenzenes with a short alkyl chain were chosen as sample compounds as a result of a calorimetric analysis of the thermal stability of the C<sub>18</sub>-silica gel particles in an atmosphere of nitrogen. Their boiling point at atmospheric pressure is less than ca. 410 K.

**Apparatus.** For the liquid–solid adsorption systems, pulse-response curves (i.e., elution peaks in chromatography) corresponding to small concentration pulses or perturbations were measured, using a high-performance liquid-chromatograph system (LC-6A, Shimadzu, Kyoto, Japan). A small volume of the sample solutions (ca. 1–5  $\mu\text{L}$ ) was introduced into the mobile-phase stream with a valve (model-7125, Rheodyne, Cotati, CA). A thermostated water bath was used to keep the column temperature constant. The concentration of the sample compounds in the column effluent was monitored with the ultraviolet detector of the HPLC system.

Similarly, pulse-response experiments were made with the gas–solid adsorption system, using a GC-9A gas chromatograph (Shimadzu, Kyoto, Japan), equipped with a thermal conductivity detector (TCD). A soap film flowmeter was used to measure the carrier gas flow rate at the detector outlet. The vapor of the sample compound was injected into the carrier gas stream at the column inlet with a gastight syringe. The injection volume depended on the sensitivity and volatility of the sample compounds and was mostly 100–200  $\mu\text{L}$ . The concentration profile of the sample compound in the effluent was monitored using the TCD. The column was placed in an oven to keep its temperature constant.

**Procedure.** The experimental conditions are listed in Table 1. Pulse-response experiments in the liquid–solid systems were carried out at near-zero surface coverage of the sample compounds while changing the column temperature between 288 and 308 K and the volumetric flow rate of the mobile phase between 1 and 2  $\text{cm}^3 \text{min}^{-1}$ . The values of  $\epsilon_p$  and  $\epsilon$  were derived from the pulse-response data measured for uracil and sodium nitrate, both inert tracers. The elution volume of uracil is equal to the volume of mobile phase inside the column, i.e., to the sum of the extraparticle and the intraparticle pore volumes because uracil can penetrate into all the pores. The total column porosity is derived from the elution time of uracil. On the other

hand, sodium nitrate ions are prevented by the Donnan salt-exclusion effect from penetrating into the intraparticle pores when a small amount of sodium nitrate is injected into the column. The external porosity ( $\epsilon$ ) of the column is thus derived from the elution time of sodium nitrate. The internal porosity ( $\epsilon_p$ ) is derived from the total and the external porosities.

For the gas–solid systems, the chromatographic peaks were also eluted at near-zero surface coverage. The column temperature was changed between 313 and 418 K. The volumetric flow rate of carrier gas was set between 0.5 and 1.0  $\text{cm}^3 \text{s}^{-1}$  (NTP).

**Data Analysis.** The required information regarding the adsorption equilibrium and the mass-transfer kinetics was derived from the first absolute moment ( $\mu_1$ ) and the second central moment ( $\mu_2'$ ) of the elution peaks, respectively, using the moment analysis method.<sup>21,32</sup> The first two moments of these peaks are formulated as follows

$$\mu_1 = \frac{\int C_e(t) t dt}{\int C_e(t) dt} = \frac{z}{u_0} \delta_0 \quad (1)$$

$$\mu_2' = \frac{\int C_e(t)(t - \mu_1^2) dt}{\int C_e(t) dt} = \frac{2z}{u_0} (\delta_{ax} + \delta_f + \delta_d) \quad (2)$$

where

$$\delta_0 = \epsilon + (1 - \epsilon)(\epsilon_p + \rho_p K) \quad (3)$$

$$\delta_{ax} = \left( \frac{\epsilon D_L}{u_0^2} \right) \delta_0^2 \quad (4)$$

$$\delta_d = (1 - \epsilon) \left( \frac{R_p^2}{15 D_e} \right) (\epsilon_p + \rho_p K)^2 \quad (5)$$

$$\delta_f = (1 - \epsilon) \left( \frac{R_p}{3 k_f} \right) (\epsilon_p + \rho_p K)^2 \quad (6)$$

where  $C_e(t)$  is the concentration of the sample compound in the mobile phase solvent leaving from the column as a function of  $t$ ,  $t$  the time,  $z$  the longitudinal distance along a column,  $u_0$  the superficial velocity of the mobile phase,  $\delta_{ax}$ ,  $\delta_f$ , and  $\delta_d$  the contributions to  $\mu_2'$  of the axial dispersion, external (fluid-to-particle) mass transfer, and intraparticle diffusion, respectively,  $\rho_p$  the density of the packing material,  $K$  the adsorption equilibrium constant,  $D_L$  the axial dispersion coefficient,  $R_p$  the particle radius,  $k_f$  the external mass-transfer coefficient, and  $D_e$  the intraparticle diffusivity. The moment analysis method was previously discussed,<sup>1,16,33–37</sup> so only basic information is presented below.

**Outline.** The value of the adsorption equilibrium constant ( $K$ ) is derived from  $\mu_1$  of the elution peak. As described earlier, the values of  $\epsilon$  and  $\epsilon_p$  (hence the phase ratio,  $\{(1 - \epsilon)(1 - \epsilon_p)\}/\{\epsilon + (1 - \epsilon)\epsilon_p\}$ ) were derived from the moments of the elution peaks of the inert tracers. The relative standard deviation of the measurements of  $\mu_1$  for the sample compounds and for the inert tracer was usually smaller than ca. 1%. Although in this study the mobile-phase flow rate was changed by a factor two, for each compound the same values of  $K$  were derived at all flow rates. This confirms that the column temperature was properly set and controlled in both gas–solid and liquid–solid experiments and at the different mobile-phase flow velocities used.



The intraparticle diffusivity ( $D_e$ ) and the axial dispersion coefficient are derived from  $\mu_2'$  after subtracting the contributions of the external mass transfer to band spreading. The relative standard deviation of the measurements of  $\mu_2'$  ranged between ca. 1% and several percent. The external mass-transfer coefficient ( $k_f$ ) of the gas–solid and RPLC systems was derived from the equations of Carberry<sup>38</sup> and Wilson–Geankoplis,<sup>39</sup> respectively.<sup>16</sup> The equation of Wilke–Chang was used to estimate  $D_m$  in aqueous methanol.<sup>1,16,40–42</sup> The values of  $D_m$  in aqueous acetonitrile and THF were derived from the Perkins–Geankoplis equation because no information is available for the association coefficient of the two organic modifiers.<sup>40</sup> The values of  $D_m$  for the sample compounds in pure acetonitrile and THF and in water were derived from the Scheibel and the Hayduk–Laudie equations, respectively.<sup>40</sup> For gas–solid systems, it is predicted that Knudsen rather than molecular diffusion is the rate-controlling process. Knudsen diffusivity ( $D_k$ ) was calculated by the Knudsen equation.<sup>16,41,42</sup> The contribution to  $\mu_2'$  of the actual adsorption/desorption kinetics at the actual adsorption sites was assumed to be negligibly small in both the gas–solid and the RPLC systems.<sup>23,37</sup> It was also assumed that intraparticle diffusion consists of two parallel contributions, those of pore and surface diffusion.<sup>16,37</sup> The value of  $D_s$  was calculated by subtracting the contribution of pore diffusivity ( $D_p$ ) from  $D_e$ . The value of  $D_p$  was estimated from  $D_m$  (RPLC systems) or  $D_k$  (gas–solid system),  $\epsilon_p$  of the C<sub>18</sub>-silica gel particles, and the tortuosity factor ( $k$ ) of the internal pores.

**Corrections.** Several corrections must be made to obtain accurate values of the adsorption equilibrium and mass-transfer kinetics parameters. The original experimental data on band retention and dispersion include the influence on  $\mu_1$  and  $\mu_2'$  of the extra-column volumes (i.e., tubings between injection valve and column and between column and detector). The true values of  $\mu_1$  and  $\mu_2'$  were derived by correcting the experimental data for the influence of these volumes, estimated from the results of tracer experiments made without column. The influence of the sample volume on  $\mu_1$  and  $\mu_2'$  in RPLC was ignored because these perturbation pulses have a very small volume. In the gas–solid adsorption experiments, the size of the perturbation pulses is far larger (100–200  $\mu$ L). However, the retention volumes of the sample compounds, even at the highest column temperature, were 2 orders of magnitude larger than the injection volume. The experimental values of  $\mu_2'$  were about 3 orders of magnitude larger than those of the injection pulse, assumed to have a rectangular shape. Thus, it is unnecessary to correct  $\mu_1$  and  $\mu_2'$  for the contribution of the injection pulse.

To derive the surface diffusion coefficient, the contributions of other mass-transfer processes to  $\mu_2'$  must be corrected by using related kinetic parameters estimated from literature correlations. The influence of these corrections on the accuracy of the surface diffusion data must be considered. As mentioned earlier, the contribution of the external mass transfer to  $\mu_2'$  was first subtracted during the determination of  $D_e$ . Any uncertainty on the estimate of  $k_f$  affects the result of the second moment analysis. In this study,  $k_f$  was estimated by the equations of Carberry<sup>38</sup> or Wilson–Geankoplis,<sup>39</sup> in gas–solid and liquid–solid adsorption systems, respectively. Other correlations have been proposed to estimate  $k_f$ .<sup>16,42,43</sup> These equations provide values of  $k_f$  that are close. For instance, for benzene at 298 K, on stationary phase particles of 45  $\mu$ m and with a superficial velocity ( $u_0$ ) of the mobile phase (70 vol % methanol) of 0.12 cm s<sup>-1</sup>, the Wilson–Geankoplis equation gives  $k_f = 1.9 \times 10^{-2}$  cm s<sup>-1</sup>. According to the Kataoka<sup>43</sup> equation,  $k_f = 1.5 \times 10^{-2}$  cm s<sup>-1</sup> under the same conditions. These two values differ by

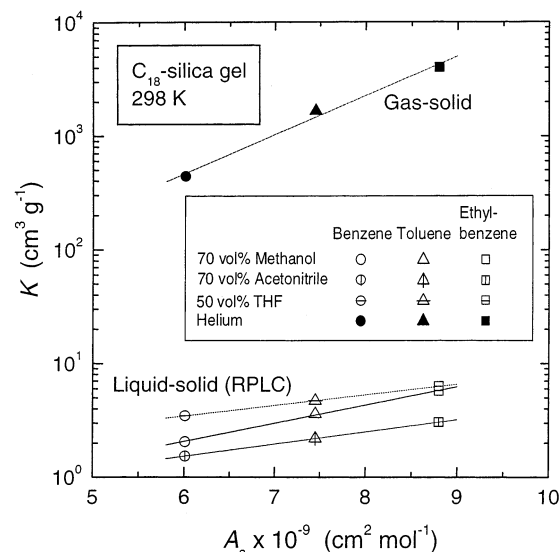


**Figure 1.** Correlation of the adsorption equilibrium constant and the hydrocarbon surface area of the sample molecules.

ca. 21–27%. Similarly, Kataoka et al.<sup>43</sup> indicate that most experimental data published agree with their correlation within an error of  $\pm 20\%$  for modified Reynolds number,  $Re' < 100$ .<sup>43</sup> As shown later, the contribution of external mass transfer to  $\mu_2'$  is negligibly small in gas–solid systems and is approximately 20–30% in RPLC systems.<sup>21,22</sup> The results of this study are only slightly influenced by small variations in the estimated value of  $k_f$ .

Finally, the contribution of intraparticle diffusion to  $\mu_2'$  was separated from that of axial dispersion by taking advantage of their different dependence on the flow rate of the mobile phase.  $D_s$  was derived from  $D_e$  by subtracting the contribution of  $D_p$  to  $D_e$ . As mentioned above,  $D_p$  was derived from  $D_m$  or  $D_k$ ,  $\epsilon_p$ , and  $k$ . The accuracy of the estimate of  $D_m$  or  $D_k$  affects that of  $D_s$ . In this study, the values of  $D_k$  were calculated using the Knudsen formula in gas systems.<sup>16,37,41,42</sup>  $D_m$  was estimated by the Wilke–Chang equation or by the Perkins–Geankoplis, Scheibel, and Hayduk–Laudie equations in RPLC systems.<sup>1,16,40–42</sup> The average error on the estimate of  $D_m$  usually ranged between 10 and 20%.<sup>40</sup> For instance, the Wilke–Chang equation gives for benzene in 70% v/v methanol, at 298 K,  $D_m = 8.2 \times 10^{-6}$  cm<sup>2</sup> s<sup>-1</sup>. The other three equations give  $D_m = 9.1 \times 10^{-6}$  cm<sup>2</sup> s<sup>-1</sup> under the same conditions.  $D_m$  values are estimated with an error of about 10%. As shown later, the contribution of surface diffusion to the overall mass transfer in C<sub>18</sub>-silica gel particles is much larger than that of pore diffusion. Most sample molecules migrate across the intraparticle space by surface diffusion. Because of the major contribution of surface diffusion, the influence of small variations in  $D_p$  (hence in  $D_m$  or  $D_k$ ) on the estimate of  $D_s$  is small. The error made in estimating  $D_m$ ,  $D_k$ , and  $D_p$  influences little the results of this study. In conclusion, reasonably accurate results were derived for the adsorption equilibrium and surface diffusion in the gas–solid and liquid–solid systems studied.

## Results and Discussion

**Adsorption Equilibrium.** Figure 1 shows the correlation between  $K$  derived from  $\mu_1$  in liquid–solid adsorption (RPLC) and the surface area of the hydrocarbon molecules ( $A_s$ ) studied. The value of  $A_s$  was calculated by summing up the surface area increments of each group in the molecule.<sup>44</sup> The logarithm of  $K$  increases linearly with increasing  $A_s$ . The slope of these lines is the methylene selectivity. It is higher for aqueous methanol than for the other two organic modifiers studied.

The linear correlation between  $\ln K$  and  $A_s$  is accounted for by the solvophobic theory.<sup>2,5–8,21</sup> The free-energy change due to the adsorption of the sample molecules in liquid–solid systems ( $\Delta G_{\text{liq}}$ ) is given by

$$\Delta G_{\text{liq}} = \Delta G_{\text{gas}} - \Delta G_{\text{vdw},s} + \frac{N_A(\lambda - 1)\mu_s^2\Psi P}{2\lambda v_s} - N_A\Delta A\gamma - \frac{N_A A_s(\kappa^e - 1)V^{2/3}\gamma}{V_s^{2/3}} - RT \ln\left(\frac{RT}{P_0 V}\right) \quad (7)$$

where  $\Delta G_{\text{gas}}$  and  $\Delta G_{\text{vdw},s}$  are the free-energy changes due to the adsorption of a sample mole in a corresponding gas–solid system and to the van der Waals interactions between the sample and the solvent molecules, respectively. The third term in the right-hand side in eq 7 represents the electrostatic contribution to  $\Delta G_{\text{liq}}$ . The contributions to  $\Delta G_{\text{liq}}$  of the two van der Waals terms,  $\Delta G_{\text{gas}}$  and  $\Delta G_{\text{vdw},s}$ , depend on the properties of the sample molecules. However, the magnitude of the changes in the first and second terms are supposed to be comparable and these changes very nearly cancel each other for closely related molecules (they have opposite signs).<sup>5</sup> The contribution of the third term in the right-hand side of eq 7 is assumed to be negligibly small in the case of the hydrophobic interactions in RPLC systems.

The value of  $\Delta G_{\text{liq}}$  is related to  $K$  as follows

$$\Delta G_{\text{liq}} = -RT \ln K \quad (8)$$

The logarithm of  $K$  in RPLC systems is derived from eqs 7 and 8 by assuming that the molecules are spherical and by introducing the assumptions described above

$$\ln K = \frac{N_A \alpha A_s \gamma}{RT} + \frac{4.836 N_A^{1/3} (\kappa^e - 1) V^{2/3} \gamma}{RT} + \ln\left(\frac{RT}{P_0 V}\right) \quad (9)$$

where  $N_A$  is the Avogadro number,  $\gamma$  the surface tension of the solvent,  $R$  the universal gas constant,  $T$  the absolute temperature,  $\kappa^e$  an energy correction parameter for curved surfaces,  $V$  the molar volume of the solvent, and  $P_0$  the atmospheric pressure. The reduction of hydrophobic surface area due to the adsorption of the sample molecules onto the stationary phase surface ( $\Delta A$ ) in eq 7 is replaced by the product of  $\alpha$  and  $A_s$  in eq 9. The parameter  $\alpha$  is the ratio of  $\Delta A$  to  $A_s$ . In the solvophobic theory,<sup>2,5–8,13,21</sup>  $\Delta A$  is assumed to be proportional to  $A_s$ . Values of  $\alpha$  ( $= \Delta A/A_s$ ) of about 0.3–0.35 for 70% v/v methanol,<sup>21,25</sup> 0.18 for 70% v/v acetonitrile,<sup>21</sup> and 0.2 for 50% v/v THF<sup>27</sup> have been reported. Values of  $\alpha$  of ca. 0.35 in RPLC with an aqueous buffer as the mobile phase<sup>5</sup> and of 0.2–0.3 for the adsorption of organic compounds from water onto an activated carbon<sup>13</sup> were also reported. Equation 9 explains the existence of a linear correlation between  $\ln K$  and  $A_s$ . It is required accurately to determine several parameters in eq 9 and to perform a quantitative detailed analysis of the retention behavior in RPLC systems.

Figure 1 shows also the linear correlation between  $\ln K$  and  $A_s$  for the gas–solid system and compares the adsorption equilibrium data in gas–solid and liquid–solid systems. The solid symbols in Figure 1 show the  $K$  values in the gas–solid system at 298 K, obtained by extrapolating the linear van't Hoff correlations.<sup>21,22</sup> The values of  $K$  in the gas–solid system are 2–3 orders of magnitude larger than those in the RPLC systems. The influence of the mobile phase on the adsorption constant in these systems explains the difference between the  $K$  values

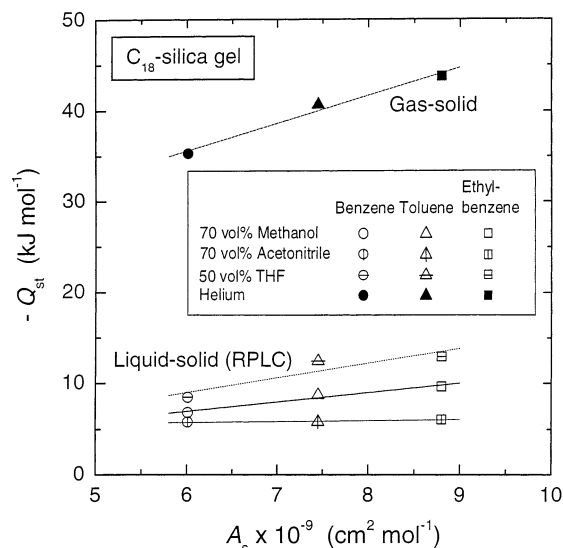


**Figure 2.** Correlation of the heat of adsorption at infinite dilution and the hydrocarbon surface area of the sample molecules.

in the two types of systems. The solvent effect on the retention behavior in RPLC has already been discussed quantitatively on the basis of the solvophobic theory.<sup>5–7,21</sup>

#### Thermodynamic Properties of Adsorption Equilibria.

According to the van't Hoff equation, the adsorption enthalpy at infinite dilution,  $Q_{\text{st}}$ , was determined from the temperature dependence of  $K$

$$K = K_0 \exp\left(\frac{-Q_{\text{st}}}{RT}\right) \quad (10)$$

where  $K_0$  is  $K$  at  $1/T = 0$  or  $|Q_{\text{st}}| = 0$ . Linear correlations were observed between the reciprocal of  $T$  and the logarithm of  $K$  of the sample compounds, i.e., benzene, toluene, and ethylbenzene, in the three RPLC and the GC systems (not shown). The values of  $-Q_{\text{st}}$  derived from the slope of these linear van't Hoff plots range from 5.8 to 13.1 kJ mol<sup>−1</sup>,<sup>21,27</sup> values that are of the same order of magnitude as other results previously reported.<sup>45–53</sup>

The values of  $Q_{\text{st}}$  thus determined are plotted against  $A_s$  in Figure 2, and straight lines are obtained. The slopes of these lines depend on the mobile-phase composition. A similar linear dependence of  $-Q_{\text{st}}$  on  $A_s$  is observed in the gas–solid system. Again, the values of  $-Q_{\text{st}}$  in the GC system are several times larger than those in the RPLC systems. The results in Figures 1 and 2 indicate that the parameters of the adsorption equilibrium and the related thermodynamics functions,  $K$  and  $-Q_{\text{st}}$ , are quite different for gas–solid and liquid–solid systems. As described earlier, a quantitative explanation of the solvent effect on  $K$  and  $Q_{\text{st}}$  in RPLC was attempted on the basis of the solvophobic theory.<sup>21</sup>

Figure 3 shows the correlation between  $K_0$  and  $Q_{\text{st}}$ . These parameters were derived as the intercept and the slope of the van't Hoff plots, respectively. Despite some scattering, Figure 3 establishes a correlation between  $\ln K_0$  and  $Q_{\text{st}}$  that is valid for all the liquid–solid and gas–solid systems. The single straight line in Figure 3 suggests that there is an enthalpy–entropy compensation (EEC) for adsorption equilibrium, irrespective of the mobile phase used, whether a solution or a gas. Numerous reports have shown an EEC for the retention behavior of various compounds in other RPLC systems<sup>21,24,27,28,30,48,54–64</sup> and demonstrated its possibility on theoretical bases.<sup>65–69</sup> Similar compensation phenomena have also

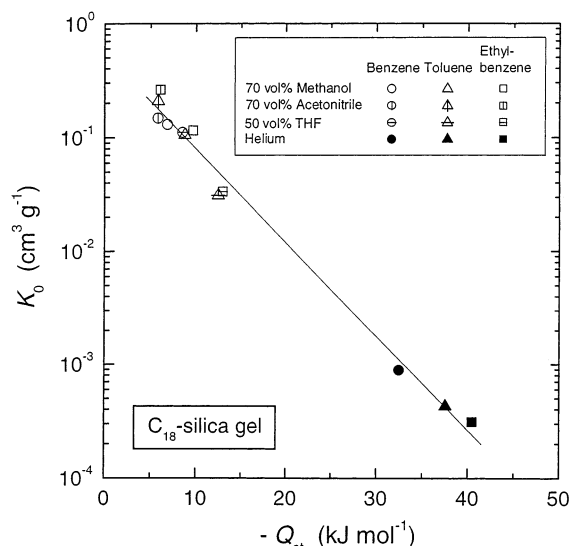


Figure 3. Enthalpy-entropy compensation of adsorption equilibrium.

been reported for the retention behavior in other systems such as ion-pair LC,<sup>70,71</sup> ion-exchange LC,<sup>72</sup> and in gas chromatography.<sup>73,74</sup>

However, Krug et al.<sup>65–67</sup> showed that linear correlations could be observed between the variations of enthalpy ( $\Delta H$ ) and entropy ( $\Delta S$ ) estimated from van't Hoff or Arrhenius plots, even when no actual EEC took place. A compensation between the errors made on  $\Delta H$  and  $\Delta S$  derived from such linear regressions leads to the apparent linear correlation between these two thermodynamic parameters. These authors pointed out that the correlation coefficient of such linear correlations could be close to unity even when the actual correlations were due to this statistical compensation effect. They also showed that, in such a case, the slope of the correlation was close to the harmonic mean of the experimental temperatures at which the measurements were made, and they proposed four different approaches in order to decide whether an observed linear correlation between  $\Delta H$  and  $\Delta S$  originates from substantially meaningful chemical or physical compensation effects or merely from the statistical pattern generated by the experimental errors.<sup>65–67</sup>

In previous papers, we quantitatively analyzed experimental data on retention equilibria in different RPLC systems using C<sub>18</sub>-silica gel and 70 vol % methanol<sup>28</sup> or 50 vol % THF<sup>27</sup> according to these four approaches. We demonstrated that the EEC observed for these retention equilibria is a true correlation. Although detailed analyses of the retention data in all other adsorption systems are required, it is likely that the linear correlation between  $\ln K_0$  and  $Q_{st}$  in Figure 3 suggests the similarity of the retention mechanism of the analytes in the gas-solid and liquid-solid systems.

**Mass-Transfer Kinetics.** The second moment analysis provides information on the mass-transfer phenomena taking place in the C<sub>18</sub>-silica gel column. It is usually assumed that  $\mu_2'$  consists of the sum of the contributions due to four kinetic processes, namely, axial dispersion ( $\delta_{ax}$ ), the external mass transfer ( $\delta_f$ ), intraparticle diffusion ( $\delta_d$ ), and the kinetics of adsorption/desorption at the actual adsorption sites ( $\delta_{ads}$ ).<sup>1,15,16</sup> However, compared with those of the other mass-transfer processes, the rate of adsorption/desorption is so fast that the influence of  $\delta_{ads}$  on band broadening is usually neglected in RPLC systems<sup>23</sup> and in other adsorption systems.<sup>37</sup> So, the second moment is given by eq 2.

Figure 4 compares the relative importance of the contributions to  $\mu_2'$  of these three kinetic processes. The total length of each

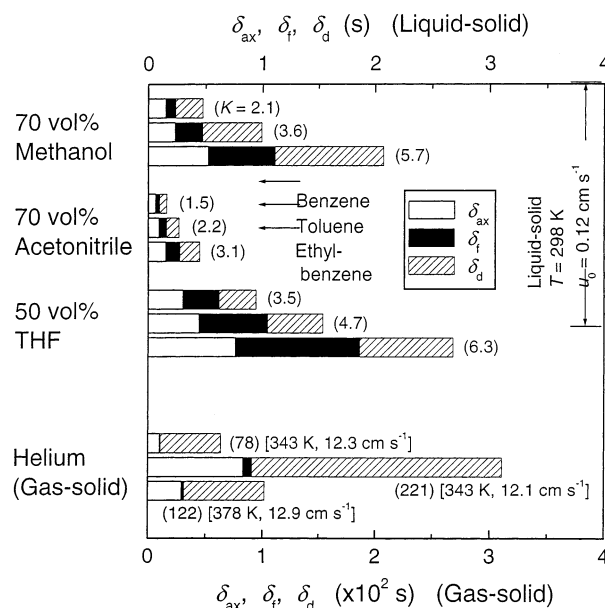


Figure 4. Comparison of the contributions of axial dispersion, external mass transfer, and intraparticle diffusion to the second central moment.

bar is approximately proportional to the value of  $K$  in the systems studied. The numbers in parentheses are the values of  $K$ . The contributions of  $\delta_{ax}$ ,  $\delta_f$ , and  $\delta_d$  are of the same order of magnitude, about 25–40%, 20–40%, and 30–50% for benzene, toluene, and ethylbenzene, respectively. Although these values depend on the mobile phase composition and the analyte, Figure 4 shows that the contributions of the three kinetic processes to peak spreading in RPLC are close when the size of the C<sub>18</sub>-silica gel particles is relatively large ( $d_p = 45$  and  $54 \mu\text{m}$  in this study). By contrast, in the gas-solid adsorption system,<sup>21,22</sup> the contribution of  $\delta_f$  is 1–2 orders of magnitude smaller than those of  $\delta_{ax}$  and  $\delta_d$ , making it negligible. The contributions of  $\delta_{ax}$  and  $\delta_d$  are approximately 15–30% and 70–80%, respectively. The numbers in brackets indicate the column temperature and the superficial velocity of the carrier gas (helium). The contribution of  $\delta_{ax}$  cannot be neglected because the reduced velocity is moderate. On the other hand, Knudsen diffusion, rather than molecular diffusion, should be the rate-controlling process in the intraparticle pores. Because the values of  $D_m$  are 1 or 2 orders of magnitude larger than those of  $D_k$ , the mass-transfer resistance contributes much to band broadening, even in the gas-solid system. Although the fractional contributions to  $\mu_2'$  of  $\delta_{ax}$ ,  $\delta_f$ , and  $\delta_d$  are different in the gas-solid and liquid-solid systems, these results show that intraparticle diffusion has a major influence on  $\mu_2'$  in all the systems studied.

It is usually assumed that the diffusive migration of the adsorbate molecules inside the intraparticle space consists of two mechanisms, pore and surface diffusion.<sup>16,37</sup> Their parallel contributions to intraparticle diffusion is represented as follows

$$D_e = D_p + \rho_p K D_s \quad (11)$$

The product  $\rho_p K D_s$  denotes the contribution of surface diffusion to intraparticle diffusion. Figure 5 compares the contributions to  $D_e$  of  $D_p$  and  $\rho_p K D_s$ . Again, the figures in parentheses and in brackets indicate the values of  $K$  and the column temperature (GC), respectively. Note that the scales are different for the LC data (top X axis) and for the GC data (bottom X axis). The value of  $D_e$  is nearly 1 order of magnitude larger than  $D_p$  in the RPLC systems, suggesting that more than 90% of the adsorbate molecules migrate across the C<sub>18</sub>-silica gel particles by way of



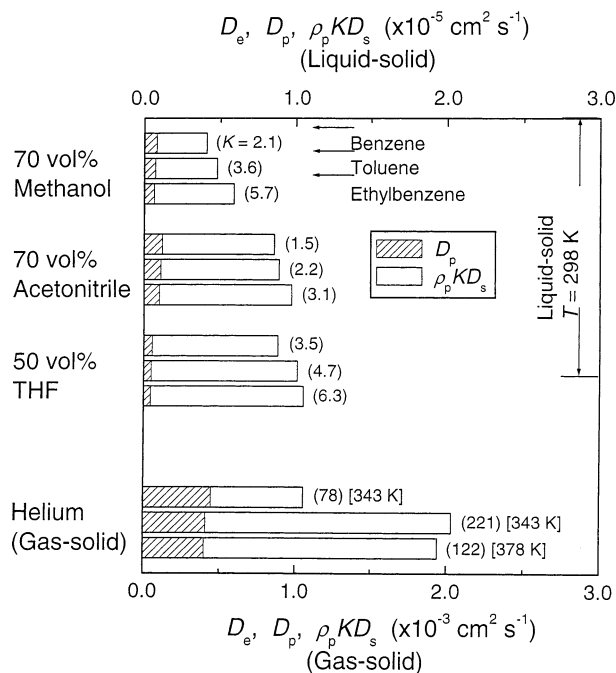


**Figure 5.** Comparison of the contributions of pore diffusion and surface diffusion to intraparticle diffusion.

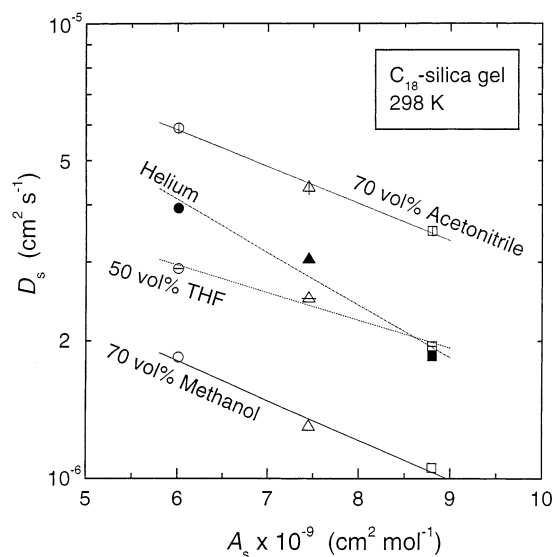


**Figure 6.** Correlation of the surface diffusion coefficient with the hydrocarbon surface area of the sample molecules. For symbols, see Figure 1.

surface diffusion. A similar situation is observed in the gas-solid adsorption system, although the orders of magnitude of the values of  $D_e$ ,  $D_p$ , and  $\rho_p KD_s$  differ by a factor of approximately 100 from those in the liquid-solid systems. The results in Figures 4 and 5 indicate that surface diffusion plays an important role in the mass-transfer kinetics across the intraparticle space and on the band broadening in  $C_{18}$ -silica gel columns, for all gas-solid and RPLC systems. A better understanding of the characteristics and the mechanism of this type of diffusive mass transfer requires a more detailed study of the surface diffusion phenomena and of the solvent effect on surface diffusion in RPLC.

**Surface Diffusion.** Figure 6 shows the correlation of  $D_s$  at 298 K in both the gas-solid and the liquid-solid systems with  $A_s$ . The solid symbols correspond to the GC system and report values of  $D_s$  at 298 K, extrapolated using the Arrhenius previously reported.<sup>21,22</sup> The values of  $D_s$  are between  $10^{-6}$  and

$10^{-5}$   $\text{cm}^2 \text{s}^{-1}$ . By contrast with the thermodynamic constants of adsorption equilibrium,  $K$  and  $-Q_{st}$  that are much larger in gas-solid than in liquid-liquid systems (see Figures 1 and 2), the experimental values of  $D_s$  determined at 298 K in either the gas-solid or the liquid-solid systems have the same order of magnitude. We discuss later whether this is physically meaningful or incidental. Figure 6 also shows that the values of  $D_s$  decrease with increasing  $A_s$  and that the logarithm of  $D_s$  is a linear function of  $A_s$ .

Figure 6 shows that the values of  $D_s$  in liquid-solid systems depend on the mobile phase composition and that the nature of the organic modifier strongly influences surface diffusion. The difference between the  $D_s$  values for the three solvents used could be explained by assuming that surface diffusion can be considered as the diffusive migration of the sample molecules through a stationary phase consisting of  $C_{18}$  alkyl ligands and molecules of the organic modifier. Tanaka et al.<sup>75</sup> demonstrated the important role of this modifier on the separation mechanism in RPLC from the viewpoints of retention equilibrium. They reported that the dependence of the retention behavior on the mobile phase composition in RPLC could be interpreted by considering that the alkyl chains associate with the organic solvent to make an effective stationary phase and that the sample molecules seem to distribute between the bulk mobile phase and this effective stationary phase.

To the best of our knowledge, other authors have reported on the characteristics of surface or lateral diffusion in surface-modified silica materials.<sup>17–20</sup> From fluorescence measurements, Bogar et al.<sup>17</sup> estimated the lateral diffusion coefficient of pyrene and the microviscosity of the phase system consisting of a  $C_{18}$  phase and a methanol/water solution (75/25, v/v). They reported that the solvated  $C_{18}$  phase is a dynamic medium in which solutes can dissolve. Wong and Harris<sup>18</sup> measured the diffusion coefficient of iodine on  $C_1$ -bonded silica in contact with methanol/water (75/25 and 50/50, v/v) solutions. Zulli et al.<sup>19</sup> measured the lateral diffusion coefficient of acridine orange at the water/ $C_{18}$  interface and compared it with the diffusivity in bulk water. Hansen and Harris<sup>20</sup> measured the diffusion coefficient of rubrene on a  $C_{18}$ -bonded phase in equilibrium with water and two methanol/water mixtures of different compositions (10/90 and 20/80, v/v). The diffusion coefficient increases with increasing methanol concentration in the aqueous solution. They reported that the values of the lateral diffusion coefficient were 2–3 orders of magnitude smaller than the molecular diffusivities in the bulk solution.

Despite these studies on surface or lateral diffusion, few papers other than ours report that  $D_s$  depends on the liquid-phase composition.<sup>18,20</sup> Most studies on surface diffusion in liquid-solid adsorption systems have so far been devoted to the adsorption of organic compounds on activated carbon or hydrophobic resins, from aqueous solutions.<sup>76</sup> The only solvent involved is water. The results of our study stress the important influence of the organic modifier on surface diffusion in RPLC.  $D_s$  increases in the following order (Figure 6): 70 vol % methanol < 50 vol % THF < 70 vol % acetonitrile. This order is quite different from that for  $K$  and  $-Q_{st}$  (Figures 1 and 2), i.e., 70 vol % acetonitrile < 70 vol % methanol < 50 vol % THF. As shown later in Figure 7, the order for  $E_s$ , i.e., 70 vol % acetonitrile < 50 vol % THF < 70 vol % methanol, is different from the previous result. However, the opposite orders for  $D_s$  and  $E_s$  reasonably correspond to each other. These results suggest that the influence of the nature of the organic solvent effect is different on surface diffusion and on the adsorption equilibrium in RPLC.

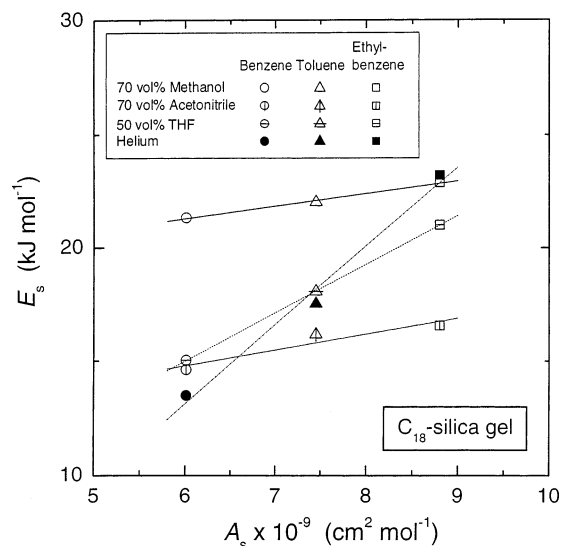


**Figure 7.** Correlation of the activation energy of surface diffusion and the hydrocarbon surface area of the sample molecules.

#### Thermodynamic Properties Concerning Surface Diffusion.

The value of  $E_s$  at near-zero surface coverage of the analytes was estimated according to the Arrhenius equation

$$D_s = D_{s_0} \exp\left(\frac{-E_s}{RT}\right) \quad (12)$$

where  $D_{s_0}$  is the frequency factor of surface diffusion. Linear correlations were observed between  $\ln K$  and  $1/T$  for the three compounds studied, in the three RPLC and the GC systems (not shown). The values of  $E_s$  calculated from the slopes of these linear Arrhenius plots are between ca. 15 and 23 kJ mol<sup>-1</sup>.<sup>21,27</sup> Figure 7 shows the plots of  $E_s$  vs  $A_s$ . Although the plots in Figure 7 exhibit a slight scatter, these plots show that  $E_s$  increases almost linearly with increasing  $A_s$ . The increment of  $E_s$  per methylene unit depends on the mobile phase composition. The values observed for  $E_s$  in Figure 7, as those for  $D_s$  in Figure 6, are of the same order of magnitude for gas–solid and liquid–solid systems. However, it remains unclear whether this is a mere coincidence or a general physical result. It is surprising that the nature of the mobile phase has such a little influence on the mass-transfer kinetics and on its parameters,  $D_s$  and  $E_s$ , while it has an extremely large effect on the equilibrium parameters,  $K$  and  $Q_{st}$ . There are few theoretical publications to explain why it should be so, although the solvent effect on  $K$  and  $Q_{st}$  was quantitatively interpreted on the basis of the solvophobic theory as described earlier.<sup>5–7,21</sup> It is expected that a detailed analysis of the influence of the nature of the organic modifier on  $D_s$  and  $E_s$  could provide some information on the characteristics and mechanism of surface diffusion.

Corresponding to Figure 3, Figure 8 shows the correlation between  $D_{s_0}$  and  $E_s$ . These two parameters were derived from the intercept and slope of the linear Arrhenius plots, respectively. Figure 8 shows that the same linear correlation between  $\ln D_{s_0}$  and  $E_s$  applies to the gas–solid and the liquid–solid systems, suggesting that there is also an EEC for surface diffusion on C<sub>18</sub>-silica gel.<sup>21</sup> As described earlier, Krug et al.<sup>65–67</sup> claimed that a rigorous verification based on their four approaches is necessary to demonstrate the linear correlation between  $\Delta H$  and  $\Delta S$ , since these parameters were estimated from linear regressions such as the van't Hoff and the Arrhenius plots. By use of these four approaches, we analyzed quantitatively the surface diffusion data and the equilibrium parameters of the RPLC

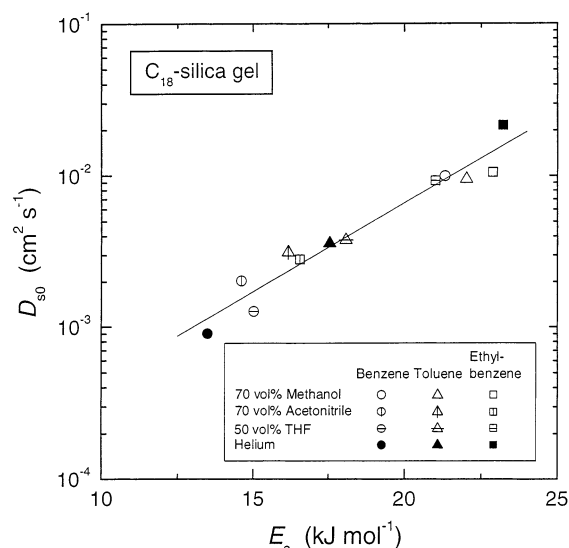


**Figure 8.** Enthalpy–entropy compensation of surface diffusion.

systems obtained with C<sub>18</sub>-silica gel and 70 vol % methanol<sup>28</sup> or 50 vol % THF.<sup>27</sup> We concluded that a linear correlation between  $\ln D_{s_0}$  and  $E_s$  (Figure 8) accounts probably for a true EEC concerning surface diffusion and originating from actual physicochemical effects taking place in the RPLC systems.

The establishment of an EEC implies that molecular migration by surface diffusion is governed by a single mechanism. It is likely that this mechanism is essentially similar, independent of the nature of the mobile phase, in gas–solid and liquid–solid adsorption systems, because all the experimental data,  $\ln D_{s_0}$  and  $E_s$ , is correlated by the same straight line. A unique interpretation should be provided for the characteristics and mechanism of surface diffusion in both the gas–solid and RPLC systems. We studied the dependence of  $D_s$  in RPLC on the retention as well as on both the adsorbate concentration and temperature.<sup>21,23,29</sup> The value of  $D_s$  tends toward the corresponding value of  $D_m$  with decreasing adsorption energy of the analyte on the stationary phase. The variations of  $D_s$  depend mostly on those of  $D_m$ . There is an intimate correlation between surface and molecular diffusion.<sup>29</sup> Surface diffusion should be considered as molecular diffusion restricted by the adsorptive interactions in the potential field of adsorption. We derived a surface-restricted molecular diffusion model as a first approximation to explain the mechanism of surface diffusion in RPLC and formulated this new model on the basis of the absolute rate theory.<sup>21,24,25,28,30</sup>

#### Interpretation of the Solvent Effect on Kinetic and Thermodynamic Parameters Relating to Surface Diffusion.

In the absolute rate theory,<sup>77</sup> the mechanism of molecular diffusion in liquid-phase systems is assumed to consist in two successive processes, a hole-making step and a jumping (or bond-breaking) step. The activation energy of molecular diffusion ( $E_m^L$ ) is thus given by

$$E_m^L = E_h^m + E_j^m \quad (13)$$

where  $E_h^m$  and  $E_j^m$  are the activation energies corresponding to the hole-making and the jumping steps, respectively. The superscripts L and m denote the mass-transfer process involved, in liquid-phase systems and molecular diffusion, respectively. It was reported that  $E_m^L$  is approximately equal to  $E_h^m$  because  $E_j^m$  is much smaller than  $E_h^m$  and is between ca. 10 and 20% of  $E_m^L$ .<sup>77</sup>



In reference to the classical model of molecular diffusion in liquid-phase systems, it is assumed in the surface-restricted molecular diffusion model that a hole is first formed by removing the proper number of solvent molecules from the potential field of adsorption. Then, a sample molecule is transferred from a neighbor adsorption site into this hole. As for molecular diffusion, the activation energy of surface diffusion in liquid–solid adsorption systems ( $E_s^L$ ) is assumed to consist in two contributions, those of the hole-making step ( $E_h^s$ ) and the jumping (bond-breaking) step ( $E_j^s$ )

$$E_s^L = E_h^s + E_j^s \quad (14)$$

where the superscript s denotes surface diffusion. The transfer of a sample molecule into the hole is assumed to require the temporary gain of the activation energy, which is necessary to break the adsorptive interactions between the sample molecule and the stationary phase. By contrast with the case of molecular diffusion,  $E_j^s$  is not negligible compared to  $E_h^s$ . The value of  $E_j^s$  is correlated with the adsorption enthalpy at infinite dilution,  $Q_{st}$

$$E_s^L = E_h^s + \beta(-Q_{st}) \approx E_m^L + \beta(-Q_{st}) \quad (15)$$

Equation 15 suggests that  $E_s^L$  is the sum of  $E_h^s$  and the contribution of the adsorption interactions, accounted for by  $\beta(-Q_{st})$ . In previous papers,<sup>21,24,25</sup>  $E_h^s$  for 70 vol % methanol was estimated at about 17–21 kJ mol<sup>-1</sup>, a value similar to that of  $E_m$  or to the activation energy of viscosity. The mechanism of molecular diffusion is similar to that of viscosity although the molecules involved are different in the two types of transfer.

The value of  $\beta$  should be positive and smaller than unity. The gain of  $E_j^s$  is required for the adsorbate molecules to be partially desorbed from the surface and diffuse, but it is not necessary that  $E_j^s$  exceeds  $-Q_{st}$  because the adsorbate molecules may migrate without being completely desorbed to the bulk mobile phase. The value of  $\beta$  was estimated at 0.4–0.55 for surface diffusion in RPLC with 70% v/v methanol.<sup>21,24,25</sup> The values of  $E_s^L$  was calculated at between 22 and 26 kJ mol<sup>-1</sup> by taking  $E_h^s = 19$  kJ mol<sup>-1</sup> and  $\beta = 0.5$  because the values of  $-Q_{st}$  are between ca. 6 and 13 kJ mol<sup>-1</sup>, as shown in Figure 2. In this model, it is assumed that the activation energy of the molecular migration without adsorptive interactions, i.e.,  $E_m$ , could be approximately converted into  $E_s$  by the addition of the contribution due to the adsorptive interactions.

If the mechanism of surface diffusion is originally similar in both the gas–solid and liquid–solid systems,  $E_s$  in the gas–solid adsorption system ( $E_s^G$ ) probably consists of the sum of the activation energy of molecular migration without adsorptive restriction ( $E_0^G$ ) and that of the adsorptive interaction, which is represented by  $\beta(-Q_{st})$ . The value of  $\beta$  is again assumed to be positive and smaller than unity

$$E_s^G = E_0^G + \beta(-Q_{st}) \quad (16)$$

The superscript G denotes a mass-transfer process in GC. In gas–solid adsorption systems, the molecular migration mechanism without adsorptive restriction would be molecular diffusion or Knudsen diffusion. The activation energies of molecular diffusion and Knudsen diffusion were respectively calculated as 3.6 and 1.4 kJ mol<sup>-1</sup> from the temperature dependence of  $D_m$  and  $D_k$ , which were conventionally estimated from the Hirshfelder equation and the Knudsen equation, respectively.<sup>16,40–42</sup> These values correspond to  $E_0^G$ .

The values of  $D_m$  and  $D_k$  in helium estimated for the analytes used in this study are of the order of  $1 \times 10^{-1}$  and  $1 \times 10^{-2}$  cm<sup>2</sup> s<sup>-1</sup>, respectively, indicating that Knudsen diffusion is the rate-controlling process. In the right-hand side of eq 16, the contribution of the first term to  $E_s^G$  is relatively small compared to that of the second term. Because the value of  $-Q_{st}$  in the gas–solid adsorption is between 35 and 44 kJ mol<sup>-1</sup> (Figure 2), the contribution of the second term to  $E_s^G$  is about 18–22 kJ mol<sup>-1</sup>, if we assume  $\beta = 0.5$ . The values of  $E_s^G$  are calculated at ca. 19–23 kJ mol<sup>-1</sup> and are close to those of  $E_s^L$  described earlier, ca. 22–26 kJ mol<sup>-1</sup>. The hypothetical calculations described above indicate that the values of  $E_s^L$  and  $E_s^G$  turn out to be similar, as shown in Figure 7, despite the difference between the contributions of  $E_h^s$  to  $E_s^L$  in eq 15 (liquid–solid adsorption) and that of  $E_0^G$  to  $E_s^G$  in eq 16 (gas–solid adsorption). Nevertheless, the mechanism of surface diffusion seems to be similar in gas–solid and liquid–solid systems.

Equation 12 is modified by combining it with eq 15 as follows

$$D_s \approx D_{s_0} \exp\left[\frac{-E_m^L - \beta(-Q_{st})}{RT}\right] \quad (17)$$

When  $D_{s_0}$  has the same order of magnitude as the frequency factor of molecular diffusion in liquid-phase systems, eq 17 can be rewritten as follows

$$D_s \approx D_m \exp\left[\frac{-\beta(-Q_{st})}{RT}\right] \quad (18)$$

In eq 18, surface diffusion is regarded as molecular diffusion restricted by adsorptive interactions between the adsorbate and the stationary phase. In liquid-phase systems, the value of  $D_m$  is usually of the order of  $1 \times 10^{-5}$  cm<sup>2</sup> s<sup>-1</sup> for the compounds used in this study. According to eq 18, the values of  $D_s$  at 298 K in the RPLC systems studied are estimated to be between ca.  $7 \times 10^{-7}$  and  $3 \times 10^{-6}$  cm<sup>2</sup> s<sup>-1</sup> by taking  $D_m = 1 \times 10^{-5}$  cm<sup>2</sup> s<sup>-1</sup> and  $\beta = 0.5$  because  $-Q_{st}$  in these RPLC systems is between ca. 6 to 13 kJ mol<sup>-1</sup>, as described earlier. These hypothetical values of  $D_s$  are in good agreement with the experimental values of  $D_s$  in Figure 6.

In analogy to eq 18,  $D_s$  could be expressed as follows

$$D_s \approx D_k \exp\left[\frac{-\beta(-Q_{st})}{RT}\right] \quad (19)$$

The values of  $D_s$  at 298 K derived from eq 19 are between ca.  $1 \times 10^{-6}$  and  $9 \times 10^{-6}$  cm<sup>2</sup> s<sup>-1</sup>, by taking  $D_k = 1 \times 10^{-2}$  cm<sup>2</sup> s<sup>-1</sup> and  $\beta = 0.5$  because the experimental values of  $-Q_{st}$  are between 35 and 44 kJ mol<sup>-1</sup> in the gas–solid system. Again, the calculated values of  $D_s$  are of the same order of magnitude as the experimental data in Figure 6. Equations 18 and 19 are based on a model considering surface diffusion as molecular migration like molecular diffusion or Knudsen diffusion, originally unrestricted by adsorptive interactions but taking place in the potential field of adsorption. When adsorbate molecules migrate in the adsorbed state, the additional adsorptive interactions restrain their mobility along the surface. Although approximate, the theoretical calculations indicate that the surface-restricted diffusion model for surface diffusion described above provides a reasonable explanation for the comparable experimental values of  $D_s$  in Figure 6 and those of  $E_s$  in Figure 7, obtained for gas–solid and liquid–solid adsorption systems.

## Conclusion

The four parameters characterizing adsorption equilibrium and surface diffusion,  $K$ ,  $Q_{st}$ ,  $D_s$ , and  $E_s$ , in gas–solid and liquid–

solid systems depend on the molecular size of the sample compounds and on the mobile phase composition. All four parameters are linearly correlated with the hydrocarbon surface area of the analytes. Whereas  $K$ ,  $-Q_{st}$ , and  $E_s$  increase with increasing  $A_s$ ,  $D_s$  decreases. In the RPLC systems,  $K$  and  $-Q_{st}$  vary similarly when the organic modifier is changed. The variations of  $D_s$  and  $E_s$  take place in a different direction than those of  $K$  and  $-Q_{st}$ . In RPLC, the influences of the solvent nature on surface diffusion and on the adsorption equilibrium are different.

Regarding the mass-transfer characteristics in  $C_{18}$ -silica gel columns, the results are different in gas–solid and in liquid–solid adsorption. The relative fractional contributions to  $\mu_2'$  of  $\delta_{ax}$ ,  $\delta_f$ , and  $\delta_d$  are different. While the contribution of  $\delta_f$  is negligible in GC, 1 or 2 orders of magnitude smaller than those of  $\delta_{ax}$  and  $\delta_d$ , none of them can be neglected in RPLC. Mass transfer in the intraparticle space has a major influence on  $\mu_2'$  in both GC and RPLC systems. The value of  $D_e$  is several times to 1 order of magnitude larger than  $D_p$  in both GC and RPLC systems, suggesting that most adsorbate molecules migrate in the  $C_{18}$ -silica gel particles by surface diffusion. Thus, surface diffusion plays an important role in intraparticle diffusion and for on-peak spreading in  $C_{18}$ -silica gel columns.

Experimental results show that the magnitude of the influence of the organic modifier on the adsorption equilibrium and its thermodynamic parameters,  $K$  and  $Q_{st}$ , is much larger than that on surface diffusion and its activation energy,  $D_s$  and  $E_s$ . The values of  $D_s$  in both GC and RPLC systems have the same order of magnitude at the same temperature. Similar values are also obtained for  $E_s$  with all the mobile phases used. Actual EECs are also observed for adsorption equilibrium and surface diffusion, illustrated by the linear correlations between  $\ln K_0$  and  $Q_{st}$  (Figure 3) and between  $\ln D_{s0}$  and  $E_s$  (Figure 8). Also, the same linear correlations between  $\ln K_0$  and  $Q_{st}$  and between  $\ln D_{s0}$  and  $E_s$  apply to GC and to RPLC results, suggesting a similarity between the adsorption equilibrium and kinetic mechanism in all forms of adsorption chromatography. Our surface-restricted diffusion model provides a quantitative explanation of the comparable values of  $D_s$  and  $E_s$  observed in GC and RPLC systems. The values of the surface diffusion coefficient derived from this model agree with the experimental ones and this explains the similar values of  $D_s$  (Figure 6) and of  $E_s$  (Figure 7) for GC and RPLC systems. This agreement also confirms the physical validity of the model.

## Glossary

$\Delta A$	reduction of total hydrocarbon surface area due to adsorption ( $\text{cm}^2 \text{mol}^{-1}$ )
$A_s$	hydrocarbon surface area of sample molecule ( $\text{cm}^2 \text{mol}^{-1}$ )
$Ce(t)$	concentration of the sample compound in the mobile phase solvent leaving from the column as a function of $t$ ( $\text{g cm}^{-3}$ )
$d_p$	particle diameter ( $\mu\text{m}$ )
$D_e$	intraparticle diffusivity ( $\text{cm}^2 \text{s}^{-1}$ )
$D_k$	Knudsen diffusivity ( $\text{cm}^2 \text{s}^{-1}$ )
$D_L$	axial dispersion coefficient ( $\text{cm}^2 \text{s}^{-1}$ )
$D_m$	molecular diffusivity ( $\text{cm}^2 \text{s}^{-1}$ )
$D_p$	pore diffusivity ( $\text{cm}^2 \text{s}^{-1}$ )
$D_s$	surface diffusion coefficient ( $\text{cm}^2 \text{s}^{-1}$ )
$D_{s0}$	frequency factor of surface diffusion ( $\text{cm}^2 \text{s}^{-1}$ )
$E$	activation energy ( $\text{kJ mol}^{-1}$ )
$E_m$	activation energy of molecular diffusion ( $\text{kJ mol}^{-1}$ )
$E_s$	activation energy of surface diffusion ( $\text{kJ mol}^{-1}$ )
$E_0$	activation energy of molecular migration without adsorptive restriction in gaseous system ( $\text{kJ mol}^{-1}$ )

$\Delta G_{\text{gas}}$	free energy change due to adsorption of sample molecule in gas–solid adsorption system ( $\text{kJ mol}^{-1}$ )
$\Delta G_{\text{liq}}$	free energy change due to adsorption of sample molecule in liquid–solid adsorption system ( $\text{kJ mol}^{-1}$ )
$\Delta G_{\text{vdw,s}}$	van der Waals interaction between sample molecule and surrounding polar solvent molecules ( $\text{kJ mol}^{-1}$ )
$\Delta H$	enthalpy change ( $\text{kJ mol}^{-1}$ )
$k$	tortuosity factor
$k_f$	external mass-transfer coefficient ( $\text{cm s}^{-1}$ )
$K$	adsorption equilibrium constant ( $\text{cm}^3 \text{g}^{-1}$ )
$K_0$	$K$ at $1/T = 0$ or $Q_{st} = 0$ ( $\text{cm}^3 \text{g}^{-1}$ )
$N_A$	Avogadro number ( $\text{mol}^{-1}$ )
$P_0$	atmospheric pressure (Pa)
$Q_{st}$	heat of adsorption at infinite dilution ( $\text{kJ mol}^{-1}$ )
$R$	gas constant ( $\text{J mol}^{-1} \text{K}^{-1}$ )
$R_p$	particle radius (cm)
$Re'$	modified Reynolds number defined as $u_0 d_p \rho / [\eta (1-\epsilon)]$
$\Delta S$	entropy change ( $\text{J mol}^{-1} \text{K}^{-1}$ )
$T$	absolute temperature (K)
$t$	time (s)
$u_0$	superficial velocity of mobile phase ( $\text{cm s}^{-1}$ )
$V$	molar volume of solvent molecule ( $\text{cm}^3 \text{mol}^{-1}$ )
$z$	column length (mm)

## Greek Symbols

$\alpha$	ratio of $\Delta A$ to $A_s$
$\beta$	ratio of $E_j^s$ to $-Q_{st}$
$\delta$	contribution of mass-transfer resistance to $\mu_2'$ (s)
$\epsilon$	external porosity of column
$\epsilon_p$	internal porosity of stationary phase particles
$\varphi$	volumetric composition of organic modifier in mobile phase solvent (%)
$\gamma$	surface tension of solvent ( $\text{N m}^{-1}$ )
$\eta$	viscosity ( $\text{Pa s}$ )
$\kappa^e$	an energy correction parameter for a curved surface
$\mu_1$	first absolute moment (s)
$\mu_2'$	second central moment ( $\text{s}^2$ )
$\rho$	density ( $\text{g cm}^{-3}$ )
$\rho_p$	particle density ( $\text{g cm}^{-3}$ )

## Subscripts

ads	actual adsorption/desorption
ax	axial dispersion
d	intraparticle diffusion
f	external mass transfer
h	hole-making process
j	jumping (bond-breaking) process

## Superscripts

G	gaseous system
L	liquid-phase system
m	molecular diffusion
s	surface diffusion

**Acknowledgment.** This work was supported in part by a Grant-in-Aids for Scientific Research (No. 12640581) from the Japanese Ministry of Education, Science and Culture, by Grant CHE-00-70548 of the National Science Foundation, and by the cooperative agreement between the University of Tennessee and the Oak Ridge National Laboratory.

## References and Notes

- (1) Guiochon, G.; Golshan-Shirazi, S.; Katti, A. M. *Fundamentals of Preparative and Nonlinear Chromatography*; Academic Press: Boston, 1994.
- (2) Krstulovic, A. M.; Brown, P. R. *Reversed-Phase High-Performance Liquid Chromatography*; John Wiley & Sons: New York, 1982.
- (3) Snyder, L. R.; Glajch, J. L.; Kirkland, J. J. *Practical HPLC Method Development*; John Wiley & Sons: New York, 1988.
- (4) Carr, P. W.; Martire, D. E.; Snyder, L. R. *J. Chromatogr. A* **1993**, 656, 1.
- (5) Horváth, C.; Melander, W.; Molnar, I. *J. Chromatogr.* **1976**, 125, 129.
- (6) Melander, W.; Horváth, C. In *High Performance Liquid Chromatography, Advances and Perspectives*; Horváth, C., Ed.; Academic Press: New York, 1980; Vol. 2, p 113.
- (7) Vailaya, A.; Horváth, C. *J. Phys. Chem. B* **1997**, 101, 5875.
- (8) Sander, L. C.; Wise, S. A. *CRC Crit. Rev. Anal. Chem.* **1987**, 18, 299.
- (9) Martire, D. E.; Boehm, R. E. *J. Phys. Chem.* **1983**, 87, 1045.
- (10) Dill, K. A. *J. Phys. Chem.* **1987**, 91, 1980.
- (11) Dill, K. A.; Naghizadeh, J.; Marquisee, J. A. *Annu. Rev. Phys. Chem.* **1988**, 39, 425.
- (12) Dorsey, J. G.; Dill, K. A. *Chem. Rev.* **1989**, 89, 33.
- (13) Belfort, G.; Altshuler, G. L.; Thallam, K. K.; Feerick, Jr., C. P.; Woodfield, K. L. *AIChE J.* **1984**, 30, 197.
- (14) Miyabe, K.; Taguchi, S.; Kasahara, I.; Goto, K. *J. Phys. Chem. B* **2000**, 104, 8481.
- (15) Giddings, J. C. *Dynamics of Chromatography, Part I, Principles and Theory*; Marcel Dekker: New York, 1965.
- (16) Ruthven, D. M. *Principles of Adsorption & Adsorption Processes*; John Wiley and Sons: New York, 1984.
- (17) Bogar, R. G.; Thomas, J. C.; Callis, J. B. *Anal. Chem.* **1984**, 56, 1080.
- (18) Wong, A. L.; Harris, J. M. *J. Phys. Chem.* **1991**, 95, 5895.
- (19) Zulli, S. L.; Kovaleski, J. M.; Zhu, X. R.; Harris, J. M.; Wirth, M. *J. Anal. Chem.* **1994**, 66, 1708.
- (20) Hansen, R. L.; Harris, J. M. *Anal. Chem.* **1995**, 67, 492.
- (21) Miyabe, K.; Guiochon, G. *Adv. Chromatogr.* **2000**, 40, 1.
- (22) Miyabe, K.; Suzuki, M. *AIChE J.* **1993**, 39, 1791.
- (23) Miyabe, K.; Guiochon, G. *Anal. Chem.* **2000**, 72, 5162.
- (24) Miyabe, K.; Guiochon, G. *J. Phys. Chem. B* **1999**, 103, 11086.
- (25) Miyabe, K.; Guiochon, G. *Anal. Chem.* **2000**, 72, 1475.
- (26) Miyabe, K.; Guiochon, G. *J. Chromatogr. A* **2000**, 903, 1.
- (27) Miyabe, K.; Sotoura, S.; Guiochon, G. *J. Chromatogr. A* **2001**, 919, 231.
- (28) Miyabe, K.; Guiochon, G. *Anal. Chem.* **2001**, 73, 3096.
- (29) Miyabe, K.; Guiochon, G. *J. Phys. Chem. B* **2001**, 105, 9202.
- (30) Miyabe, K.; Guiochon, G. *Anal. Chem.* **1999**, 71, 889.
- (31) Awum, F.; Narayan, S.; Ruthven, D. *Ind. Eng. Chem. Res.* **1988**, 27, 1510.
- (32) Miyabe, K.; Guiochon, G. *J. Sep. Sci.* **2003**, 26, 155.
- (33) Kucera, E. *J. Chromatogr.* **1965**, 19, 237.
- (34) Kubin, M. *Collect. Czech Chem. Commun.* **1965**, 30, 2900.
- (35) Grushka, E.; Myers, M. N.; Schettler, P. D.; Giddings, J. C. *Anal. Chem.* **1969**, 41, 889.
- (36) Grushka, E. *J. Phys. Chem.* **1972**, 76, 2586.
- (37) Suzuki, M. *Adsorption engineering*; Kodansha/Elsevier: Tokyo/Amsterdam, 1990.
- (38) Carberry, J. J. *AIChE J.* **1960**, 6, 460.
- (39) Wilson, E. J.; Geankoplis, C. J. *Ind. Eng. Chem. Fundam.* **1966**, 5, 9.
- (40) Reid, R. C.; Prausnitz, J. M.; Sherwood, T. K. *The Properties of Gases and Liquids*; McGraw-Hill: New York, 1977.
- (41) Treybal, R. E. *Mass-Transfer Operations*; McGraw-Hill: New York, 1980.
- (42) Bird, R. B.; Stewart, W. E.; Lightfoot, E. N. *Transport Phenomena*; John Wiley & Sons: New York, 2002.
- (43) Kataoka, T.; Yoshida, H.; Ueyama, K. *J. Chem. Eng. Jpn.* **1972**, 5, 132.
- (44) Bondi, A. *J. Phys. Chem.* **1964**, 68, 441.
- (45) Knox, J. H.; Vasvari, G. *J. Chromatogr.* **1973**, 83, 181.
- (46) Colin, H.; Guiochon, G. *J. Chromatogr.* **1977**, 141, 289.
- (47) Colin, H.; Guiochon, G. *J. Chromatogr.* **1978**, 158, 183.
- (48) Colin, H.; Diez-Masa, J. C.; Guiochon, G.; Czajkowska, T.; Miedziak, I. *J. Chromatogr.* **1978**, 167, 41.
- (49) Horváth, C.; Melander, W. *J. Chromatogr. Sci.* **1977**, 15, 393.
- (50) Issaq, H. J.; Jaroniec, M. *J. Liq. Chromatogr.* **1989**, 12, 2067.
- (51) Alvarez-Zepeda, A.; Barman, B. N.; Martire, D. E. *Anal. Chem.* **1992**, 64, 1978.
- (52) Guillaume, Y. C.; Guinchard, C. *Anal. Chem.* **1996**, 68, 2869.
- (53) Guillaume, Y. C.; Guinchard, C. *Anal. Chem.* **1997**, 69, 183.
- (54) Melander, W. R.; Campbell, D. E.; Horváth, C. *J. Chromatogr.* **1978**, 158, 215.
- (55) Melander, W. R.; Chen, B. K.; Horváth, C. *J. Chromatogr.* **1979**, 185, 99.
- (56) Melander, W. R.; Stoveken, J.; Horváth, C. *J. Chromatogr.* **1980**, 199, 35.
- (57) Melander, W. R.; Mannan, C. A.; Horváth, C. *Chromatographia* **1982**, 15, 611.
- (58) Melander, W. R.; Horváth, C. *Chromatographia* **1984**, 19, 353.
- (59) Vigh, G.; Varga-Puchony, Z. *J. Chromatogr.* **1980**, 196, 1.
- (60) Jinno, K.; Ohshima, T.; Hirata, Y. *J. High Resolut. Chromatogr. Chromatogr. Commun.* **1981**, 4, 466.
- (61) Jinno, K.; Ohshima, T.; Hirata, Y. *J. High Resolut. Chromatogr. Chromatogr. Commun.* **1982**, 5, 621.
- (62) Kuchar, M.; Rejholec, V.; Miller, V.; Kraus, E. *J. Chromatogr.* **1983**, 280, 289.
- (63) Kuchar, M.; Kraus, E.; Rejholec, V.; Miller, V. *J. Chromatogr.* **1988**, 449, 391.
- (64) Woodburn, K. B.; Lee, L. S.; Rao, P. S. C.; Delfino, J. J. *Environ. Sci. Technol.* **1989**, 23, 407.
- (65) Krug, R. R.; Hunter, W. G.; Grieger, R. A. *J. Phys. Chem.* **1976**, 80, 2335.
- (66) Krug, R. R.; Hunter, W. G.; Grieger, R. A. *J. Phys. Chem.*, **1976**, 80, 2341.
- (67) Krug, R. R. *Ind. Eng. Chem. Fundam.* **1980**, 19, 50.
- (68) Boots, H. M. J.; de Bokx, P. K. *J. Phys. Chem.* **1989**, 93, 8240.
- (69) Vailaya, A.; Horváth, C. *J. Phys. Chem.* **1996**, 100, 2447.
- (70) Riley, C. M.; Tomlinson, E.; Jefferies, T. M. *J. Chromatogr.* **1979**, 185, 197.
- (71) Riley, C. M.; Tomlinson, E.; Hafkenscheid, T. L. *J. Chromatogr.* **1981**, 218, 427.
- (72) de Bokx, P. K.; Boots, H. M. J. *J. Phys. Chem.* **1989**, 93, 8243.
- (73) Kuchar, M.; Tomkova, H.; Rejholec, V.; Korhonen, I. O. O. *J. Phys. Chem.* **1987**, 398, 43.
- (74) Li, J.; Carr, P. W. *J. Chromatogr. A* **1994**, 670, 105.
- (75) Tanaka, N.; Kimata, K.; Hosoya, K.; Miyanishi, H.; Araki, T. *J. Chromatogr. A* **1993**, 656, 265.
- (76) Kapoor, A.; Yang, R. T.; Wong, C. *Catal. Rev. — Sci. Eng.* **1989**, 31, 129.
- (77) Glasstone, S.; Laidler, K. J.; Eyring, H. *The Theory of Rate Processes*; McGraw-Hill: New York, 1964.